Clinical Anatomy 4:433–446 (1991)

Imaging the Thoracic Lymphatics: Experimental Studies of Swine

JAMES D. COLLINS, MARLA L. SHAVER, ANTHONY C. DISHER, POONAM BATRA, KATHLEEN BROWN, AND THEODORE Q. MILLER

Department of Radiological Sciences, UCLA School of Medicine (J.D.C., M.L.S., P.B., K.B.), and Department of Radiology, Charles R. Drew Postgraduate School of Medicine (A.C.D., T.Q.M.), Los Angeles

The lungs and hearts of 15 swine were surgically harvested intact and studied in the fresh state. The lymphatics of the lung and mediastinum were cannulated and contrast medium was introduced by retrograde injection to identify the visceral pleural lymphatics and deep lymphatics of the lung. Radiographic x-ray, CT, MR, and color photographic images were obtained. Collateralization, extravasation (bronchorrhea), perivascular stasis, and circumvention were demonstrated. Lymphatic communication with the contralateral lung, thoracic duct, heart, and the diaphragm was demonstrated. The findings correlate with the lymphangiographic display of lymphedema of the extremities, obstruction to lymph flow secondary to congenital abnormalities, trauma, tumor, and infections. Our results support the view that stents and/or large bore needles may be introduced into the superficial lymphatics of the lung. The lymphatics of the lung may be anastomosed post lung transplantation and thus possibly reduce passive congestion that occurs in the early postoperative period. The authors postulate that tumor cells and infectious agents may be spread from one lung to the other by the anatomical pathways demonstrated.

Key words: MRI, pulmonary ligament, ethiodol oil, heart lung model, transplantations, lymphangiogram

INTRODUCTION

The lymphatic system forms an important but elusive network whose clinical significance all too often is initially noted postoperatively because it is not appreciated intraoperatively. We have developed a method to demonstrate thoracic

Received for publication December 20, 1990; revised February 25, 1991.

Address reprint requests to James D. Collins M.D., Department of Radiological Sciences, UCLA Center for the Health Sciences, Los Angeles, CA 90024.

This work was presented at the 103rd Annual American Association of Anatomists Meeting, Philadelphia, PA, April 25, 1990 and the 96th Annual Convention of the National Medical Association, Las Vegas, Nevada, July 30, 1990.

lymphatics intraoperatively using the similarities of swine and human thoracic contents and to demonstrate how knowledge of thoracic lymphatic anatomy can be applied clinically.

General anesthetics administered to patients having surgical procedures will decrease blood pressure by relaxing the vascular system. Intravenous fluids are given to maintain normal blood pressure and stabilize vital signs during these procedures. The vascular system contracts during the postoperative period. The excess intravascular fluid will deposit into the soft tissues and pleural space. The postoperative chest radiograph may demonstrate the excess fluid as pleural effusions and obliteration of the fascial planes. The pleural effusions may be large enough to compromise oxygenation of the lung and prolong the patients' hospitalization time.

A review of our surgical operative reports confirms that the lymphatic channels are not tied off or reunited when patients have lobectomies, pneumonectomies, liver transplants, and/or transplants of the heart and lung. However, the renal transplant patients have the lymphatics tied off to prevent lymphocele formation which may contribute to vascular compromise. Methylene blue is used to identify the lymph channels in renal transplant patients to avoid lymphocele formation. Cannulation of the lung lymphatics is possible because stents and smaller tubes can be inserted into the pulmonary lymphatics in freshly harvested lungs. Thus, the united lymphatics would reduce the loss of electrolytes, lymph fluid, and decrease pulmonary edema morbidity postoperatively.

Models of radiographic pathological correlation have been constructed to explain the radiographic correlation to the clinical pathology. Hoffman et al. (1966) revealed with balloons how intraluminal fluid and air could be mistaken as a sign of bowel wall separation. Collins et al. (1972a, b) found 25 ml of fluid to be the smallest effusion to measured on the upright chest radiograph, and also demonstrated the smallest detectable calcification on the plain chest radiograph. Moskowitz et al. (1973) demonstrated 5 ml as the smallest effusion measurable on the lateral decubitus chest radiograph. Studies by Collins et al. (1989) revealed how nerves are demonstrated on MRI by imaging freshly harvested brachial plexus tissue at autopsy. Since freshly harvested tissue can be imaged with magnetic resonance, a model using MRI to demonstrate cannulation of the lymphatics of the lung should be possible.

The lung pumps air, blood, and lymph fluid. The expansion of the lung compresses the vascular and lymphatic structures of the lung. Our team successfully cannulated the lung lymphatics and recorded the pulmonary lymphatics with plain radiographs and MR images. We are able to demonstrate the circulation routes over the pleural surface and the deep structures of the lung. The purpose of this research is to present the anatomy and the clinical significance for teaching and patient care.

METHODS AND MATERIALS

Fifteen swine were given preoperative ketamine and xylozine before being placed on the fluoroscopic table. An 8.0 mm endotracheal tube was inserted proximal to the division of the trachea under fluoroscopic control. The tube was

secured by inflating the endotracheal cuff. An Ohio ventilator was used to administer halothane for general anesthesia.

A vertical incision was then made from the level of the thyroid cartilage to approximately 6 in below the xyphoid process. Blunt dissection was performed down to the fascial planes of the neck, mediastinum, and the upper abdomen. The major blood vessels of the neck, thorax, and upper abdomen were tied off with number 4.0 silk ligatures in order to maintain a clear field of vision to harvest the lungs and heart. The esophagus and the thoracic duct were also tied off with 4.0 silk. The inferior visceral pleural reflection from the pulmonary hila to the diaphragm was preserved along with a portion of the diaphragm. This was accomplished to maintain the lymphatic drainage from the abdomen and the diaphragm. The lungs and the heart were then harvested. Sacrifice was accomplished by intravenous injection of phenobarbital and exsanguination.

The endotracheal tube was taped above the thyroid cartilage in the harvested specimen. The lungs were inflated with room air using a syringe to study the effects upon the lymphatic drainage of the visceral pleural surface and lung parenchyma with and without the injection of ethiodol oil.

Normal saline was injected selectively into the tracheal lymph nodes to identify the largest lymph channels for cannulation with Viamonte needles. The visceral pleural (surface), hilar, and the tracheal lymphatics were cannulated. The needles were then connected with K-50 tubing to a 20 cc plastic syringe. A pressure pump was used for continuous infusion of the ethiodol oil. Overhead and spot fluoroscopic films were obtained using a Philips radiographic fluoroscopic unit. Magnetic resonance images (MRI) (T1-weighted) and computerized tomography images (CT) of the harvested heart and lung specimen were obtained. Ektachrome 100 daylight film was used to obtain color slides.

RESULTS

The heart and lungs were harvested from 15 swine within 20 minutes following sacrifice. The surfaces of the lungs were very red from the pooling of blood in the capillary bed. The lymphatics, terminal bronchioles, and the vascular structures were easily identified (Fig. 1). When the lungs were inflated with room air, the red coloration changed to a yellowish orange. The vascular structures and the visceral pleural lymphatics were compressed by the expanding lungs and were grossly invisible (Fig. 2a, b). However, the surface lymphatics over the trachea and mediastinum dilated. The peritracheal and perihilar lymph nodes enlarged.

The partial inflation of the lungs accentuated the lymphatics in the interlobular septa and partially dilated the visceral pleural lymphatics. Valves, areas of constriction within the marginal visceral pleural lymphatics, were identified (Figs. 3, 5). The visceral pleura lymphatics were uniformly distributed over both lungs and were readily visible. Retrograde saline injections into the lymphatics adjacent to the right hilum (Fig. 4) increased the dilation of the lymphatics over the mediastinum and the visceral pleural surface of the lungs (Fig. 5). The lymphatics dilated at the tip of the cannula from 1.0 mm to 1.5 mm. The saline injections allowed our team to select several lymphatics for cannulation. The Viamonte needles were introduced and secured into the lymphatics over the trachea, hila,

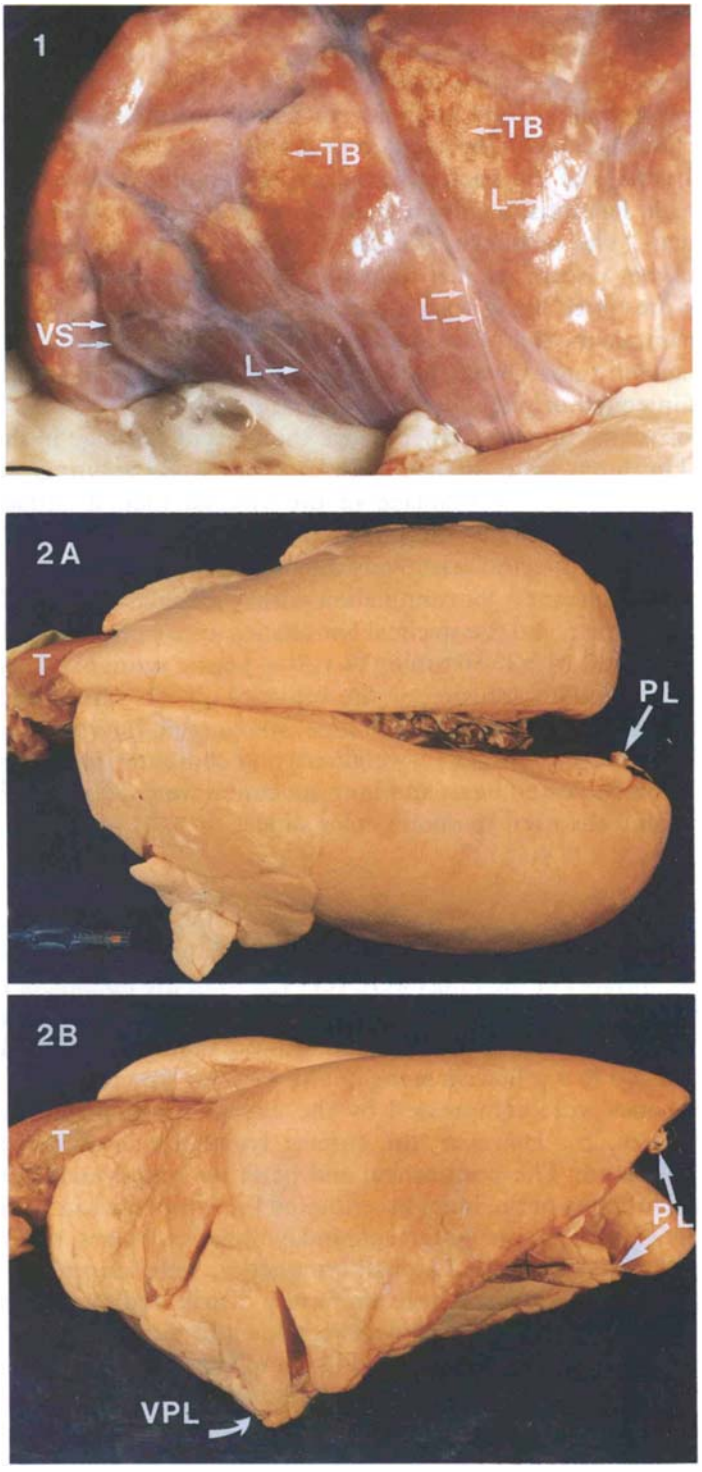

Fig. 1 (top); **Fig. 2** (A, B)

and the visceral pleural lymphatics (Fig. 5). The visceral pleural lymphatics of both lungs dilated and glistened from the reflected light after saline injections. The retrograde saline injection enlarged the mediastinal lymph nodes (Fig. 6) and the thoracic duct.

Ethiodol medium injections monitored under fluoroscopic control demonstrated filling of the visceral pleural lymphatics and lymph nodes in the unexpanded and partially expanded lungs. Continued pressure injection of ethiodol filled the peribronchial lymphatics and caused extravasation of the ethiodol into the alveoli spaces (bronchorrhea). As the lungs expanded, the peribronchial lymphatics and some of the visceral pleural lymphatics were emptied by the increased pressure of the expanding lungs (Figs. 7, 8a, b). Ethiodol contrast injections into the unexpanded lung demonstrated contiguous lymphatics, lymph nodes, and communication between both lungs. When the lungs were fully inflated, the contrast media in the contiguous lymphatics and lymph nodes decreased, and the thoracic duct filled with ethiodol (Fig. 9a, b).

Magnetic resonance images (MRI) demonstrated the fascial planes and the anatomy of the freshly harvested heart lung model. Coronal MR images post-ethiodol medium injection documented the oily ethiodol as a high signal (white) in the peribronchial lymphatics (Fig. 10a, b). Fluoroscopy and overhead radiographs best demonstrated the filling of the visceral pleural lymphatics communicating with the interlobular septal lymphatics and the peribronchial lymphatics (Fig. 11). The continuous injection of the ethiodol caused the peribronchial lymphatics to rupture. The oily ethiodol extravasation was demonstrated as a white haze and a partially interrupted white column contrast medium in the pulmonary veins (Fig. 12).

Computerized tomography (CT) was performed on the freshly harvested heart lung model and did not demonstrate contiguous anatomy that would be needed for MRI correlation. The MR images were obtained because the contiguous anatomy of the trachea and bronchi were demonstrated. The CT images were noncontributory and are not presented.

DISCUSSION

The lymphatics of the lung can be cannulated with large bore needles. The anatomy of the swine and human lymphatics is similar. Plain x-rays and MRI studies can demonstrate the thoracic lymphatics. The knowledge of the thoracic lymphatic anatomy can be useful intraoperatively to reunite lymphatics and may reduce the postoperative complications that lead to patient morbidity.

Fig. 1. Freshly harvested heart lung model. The right lung is reflected laterally from the trachea and the mediastinum demonstrating the bluish vascular structures (VS) as they course over the mediastinal fat. Terminal bronchioles, TB; translucent lymphatics, L.

Fig. 2. **A:** A dorsal view of the expanded lungs demonstrating compression of the vascular and lymphatic structures. Pulmonary ligament, PL; trachea, T. **B:** A lateral view of the expanded lungs demonstrating the lobes of the lung and the "pulmonary ligaments" (PL). Visceral pleural lymphatics, VPL; trachea, T.

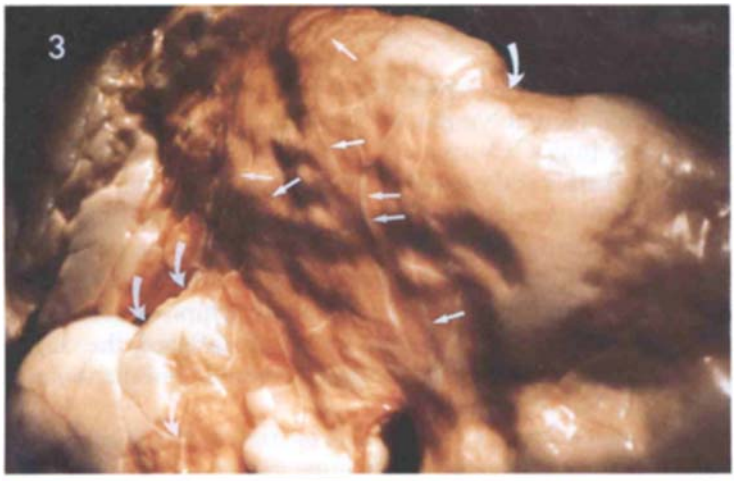

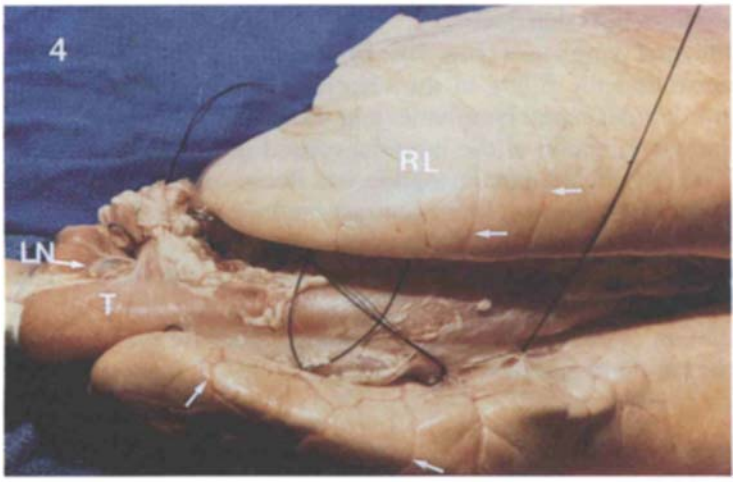

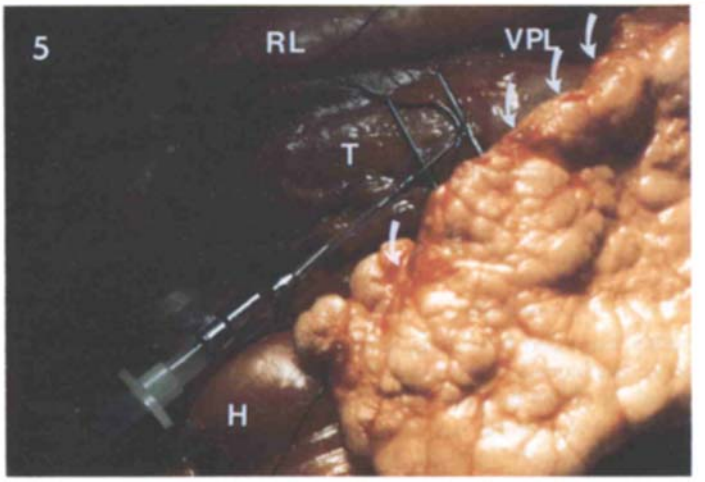

Figs. 3, 4, 5

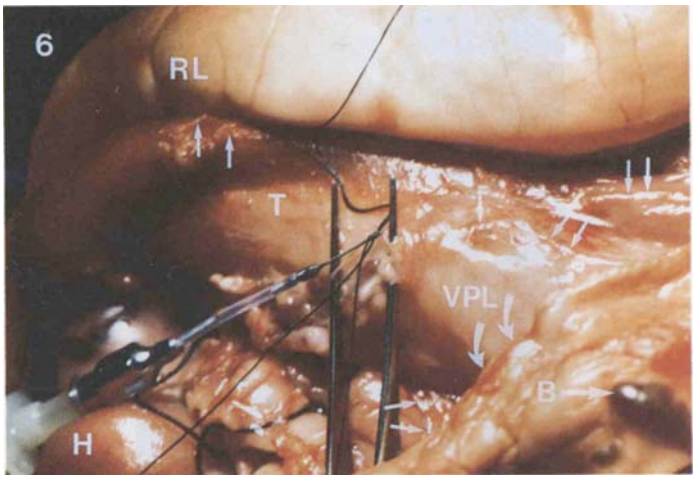

Fig. 6. This is the enlarged image of Figure 5 demonstrating dilated, glistening lymphatics (arrows) over the surface of the lung and posterior mediastinum. The curved arrows indicate the larger dilated visceral pleural lymphatics (VPL) on the edge of the left lung. Right lung, RL; trachea, T; bleb, B; heart, H.

Ontogeny correlates the embryology to the life history of an individual. Phylogeny describes the progression of a particular race or species from its simplest form to a more complex or higher form. Since many of the earlier embryological stages of man resemble the adult stages of animals in the lower phyla, it is often said that ontogeny recapitulates phylogeny. Studies by Towers (1968) eloquently stated that "similarities that exist between mammals in respect of lung structure are greater than exist in respect of any other system in the body. This is hardly surprising since this organ is engaged in chemical exchange with a gas mixture whose chemical composition varies within only very narrow limits in that small portion of the atmosphere where mammals normally live." The authors are aware that the swine lung is not exactly the same as the human lung. However, the anatomy of the swine lung has been studied for over 2,000 years and the animal is readily available from other research protocols. Therefore, it would seem logical that the swine heart lung model should be used to evaluate the lymphatic circulation of the lung.

Radiological and pathological correlation of the freshly autopsied human lung has been performed at our institution since 1967. The senior author has observed

---

Fig. 3. The partially expanded lungs with dilated lymphatics (arrows) accompany the vascular structures over the pleural surface of the lung. The visceral lymphatics (VPL) on the edge of the lung (curved arrows) measure 1.0 mm in diameter. The trachea is inferior to the lung and outside of the photograph.

Fig. 4. The black silk sutures isolate lymphatic channels over the dorsum of the lungs prior to cannulation. The interlobular septa (arrows), trachea (T), right lung (RL), and lymph node (LN) are demonstrated.

Fig. 5. An isolated lymphatic has been cannulated with the Viamonte needle over the right main stem bronchus. Trachea, T; visceral pleural lymphatics (VPL), curved arrows; right lung, RL; heart, H.

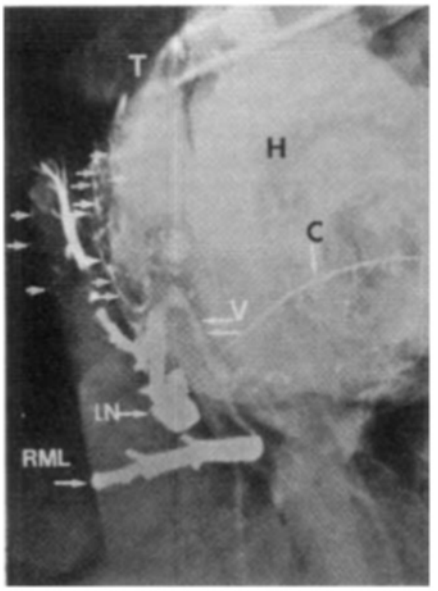

Fig. 7. Radiographic demonstration post ethiodol injection into a lymph node (ventral view) in the unexpanded lung. A reticular pattern is formed from the retrograde filling of the peribronchial lymphatics, numerous visceral pleural (small arrows) and interlobular septal lymphatics in the right upper lung. Extravasation into a vein (v) communicates contrast to the the right middle lobe bronchus (RML). Heart, H; trachea, T; lymph node, LN; catheter, C.

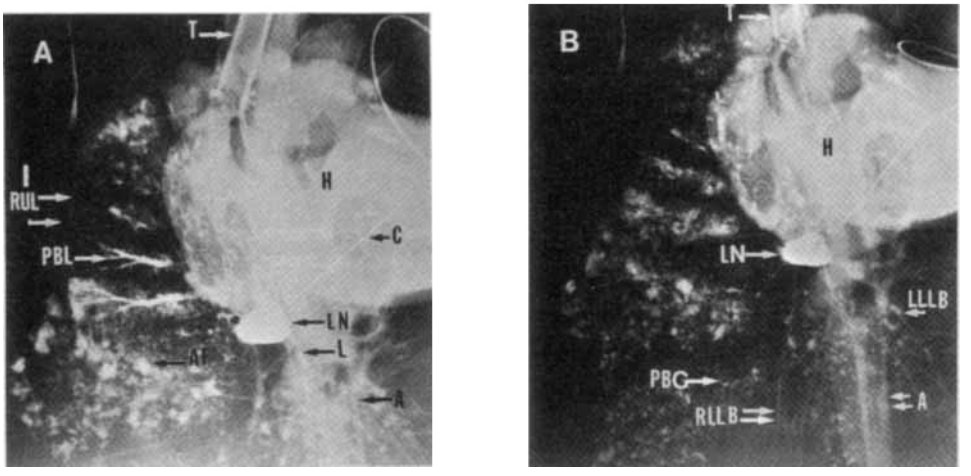

Fig. 8. **A:** Serial radiographic image of Figure 7 post injection of contrast medium demonstrating peribronchial lymphatics (PBL), visceral pleural lymphatics, and extravastation of contrast into the terminal bronchioles (bronchorrhea) of the partially expanded lung. Heart (H), lymph node (LN), trachea (T), aorta (A). **B:** Serial radiographic image post injection of contrast medium demonstrating decreased ethiodol contrast surrounding the compressed peribronchial lymphatics in the expanded lung. Aorta, A; heart, H; left lower lobe bronchus, LLLB; lymph node, LN; peribronchial cuffing, PBC; trachea, T; right lower lobe bronchus, RLLB.

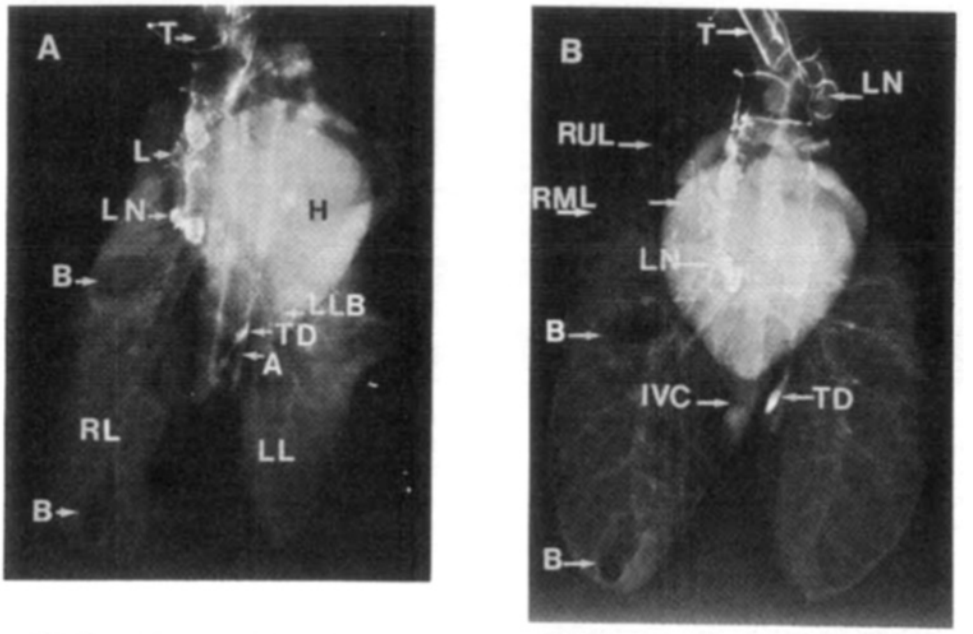

Fig. 9. **A:** A radiograph post injection of ethiodol into a right peribronchial lymphatic (L). The lungs are unexpanded. The lymphatics and contiguous lymph nodes (LN) fill with contrast. The lymphatics to the mediastinum and left lung begin to fill. Aorta, A; bleb, B; heart, H; left lung, LL; thoracic duct, TD; right lung, RL; trachea, T; **B:** A serial radiograph of heart lung model in Figure 10a demonstrating expansion of the lungs and increased ethiodol contrast in the thoracic duct (TD). Bleb, B; lymph node, LN; right middle lung, RML; right upper lung, RUL; inferior vena cava, IVC; thoracic duct, TD.

many similarities between the autopsied human lung and swine heart lung model. Studies by Miller (1947) detailed the anatomy of the canine pulmonary lymphatics. Willis (1675) illustrated the pulmonary lymphatics in the ox lung.

The gross anatomy of the autopsied human lung and the heart lung model are similar. The shape of the lungs follows the shape of the thorax. Although there is a distinct difference in shape between the swine and human lung, both are like balloons that have expanded to fill the thoracic cavity. The human lung and the swine heart lung model have visceral pleural lymphatics over the dependent edges of the lung which measure approximately 1.0 mm in diameter. Lymphatics are on both sides of the vascular structures of the visceral pleural surface of the lung. The concept that the lymphatics of the human lung could be cannulated as in the heart lung model was adopted. We informed the cardiovascular surgeons and demonstrated how the lymphatics of the lungs could be cannulated.

In an earlier report Trapnell (1963) demonstrated the "superficial" visceral pleural lymphatics of the lung in human cadaver formalin preserved lungs. He stated that the superficial lymphatics were not as numerous in the upper lung as in the lower lung. Our studies revealed numerous visceral pleural lymphatics over both lungs which communicated with the mediastinum. We observed lymphatic communication between both lungs, trachea, esophagus, aorta, thoracic duct, heart, pulmonary ligament, and the diaphragm. We also observed that the pulmo-

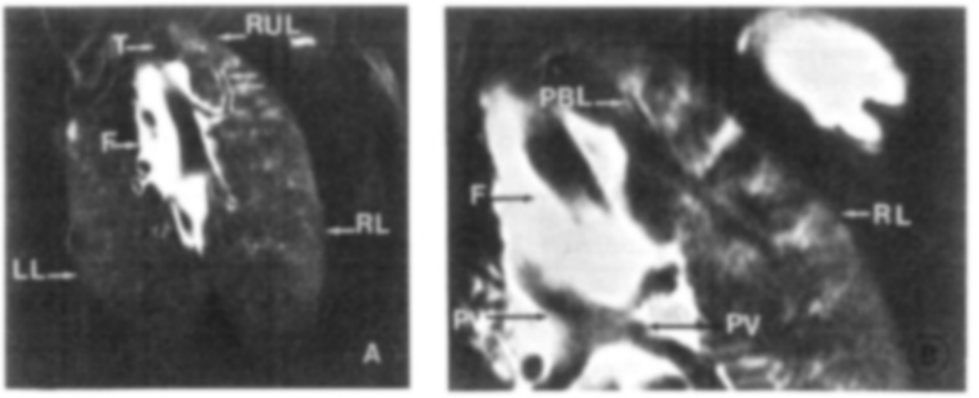

Fig. 10 **A:** A (dorsal) coronal MR image of the heart lung model post contrast injection demonstrating contiguous anatomy and contrast in the peribronchial lymphatics (two arrows) of the right upper lung. No contrast is present within the bronchial lumen. Mediastinal fat, F; left lung, LL; right lung, RL; right upper lung, RUL; trachea, T. **B:** An enlarged (dorsal) coronal MR image in Figure 9A. This section is slightly inferior to the image in Figure 9A. The pulmonary veins seem to cross as they enter the left atrium. Mediastinal fat, F; peribronchial lymphatic, PBL; pulmonary vein, PV.

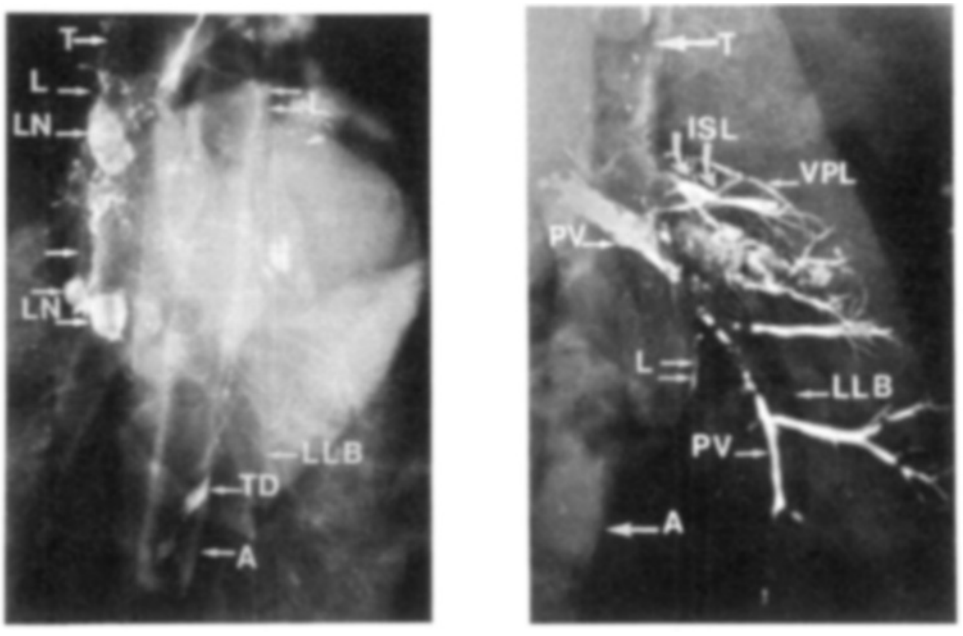

Fig. 11. This is an enlarged radiograph of Figure 9A demonstrating the intercommunication of the fine network of lymphatics (L) in the mediastinum with the peritracheal, and peribronchial lymphatics with the lymphatics of the left lung. Periaortic lymphatics, two arrows; aorta, A; lymphatic, L; lymph node, LN; left lower lung bronchus, LLB; thoracic duct, TD; trachea, T.

Fig. 12. An enlarged radiograph demonstrating the injection of ethiodol contrast into a right upper lung visceral pleural lymphatic (VPL). The interlobular septal lymphatics (ISL)(curved arrows) communicate with dilated peribronchial lymphatics. Ethiodol contrast has ruptured into the pulmonary vein (PV). Aorta, A; lymphatic in the wall of the inferior vena cava, L; trachea, T; lower lung bronchus, LLB.

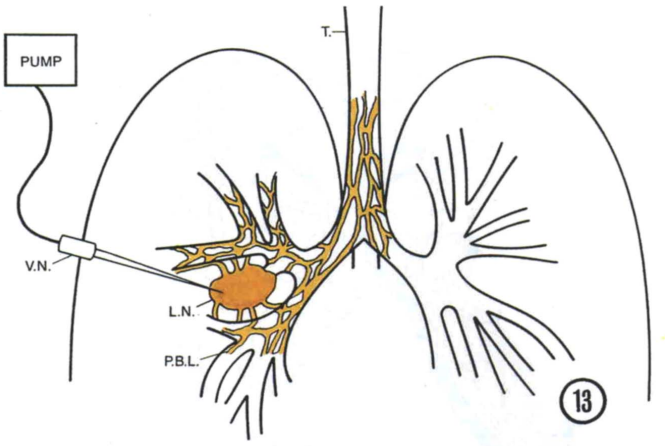

Fig. 13. A diagram illustrating a graphic representation of the heart-lung model. A Viamonte needle is in the lymph node. The heart is not demonstrated. Lymph node, LN; peribronchial lymphatics, PBL; Viamonte needle, VN; trachea, T.

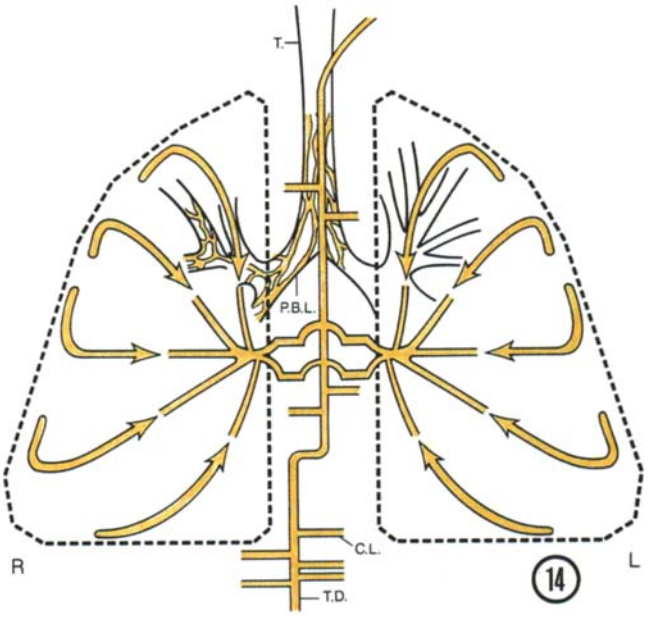

Fig. 14. A diagram illustrating thoracic lymphatics. This is a graphic illustration indicating the direction of flow of the lymphatics from the visceral pleura toward the pulmonary hila, thoracic duct (TD), collateral lymphatics (CL) communicating with the thoracic duct. The lymph nodes are not illustrated. Trachea, T; peribronchial lymphatics, PBL; mediastinum, right lung, R; left lung, L.

nary ligament is not a true ligament but a reflection of the visceral pleura containing lymphatics, small nerves, and blood vessels which provide communication between the abdomen and thorax. The pulmonary ligament often is cut in surgical resections of the lung. The reader should recall that the normal flow of lymph fluid is from the abdomen toward the chest. In patients who suffer trauma to the

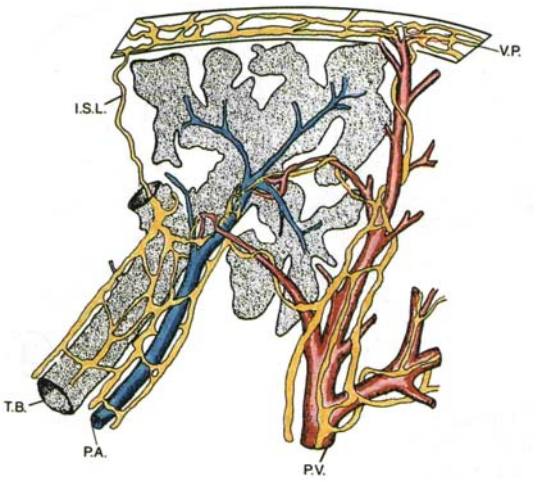

Fig. 15. A diagram demonstrating the lymphatic drainage of a portion of a lung lobule and the visceral pleura (VP). Interlobular septal lymphatic, ISL; pulmonary artery, PA; pulmonary vein, PV; terminal bronchiole, TB.

abdomen chyle may accumulate in the pleural space, illustrating the direction of lymph flow. We have had three cases where chyle appeared in the right pleural space after trauma to the abdomen from auto accidents. In an earlier report (Weidner and Steiner, 1971) ethiodol refluxed into dilated intrapulmonary lymphatics and extravasated into the pleural space. The report indicated the pulmonary valves were incompetent. It has been very common in our experience to see ethiodol circumvent on a normal lymphangiogram into the lymphatics of the mediastinum, cervical lymph nodes, and axillary lymph nodes. The mechanical pumping of the ethiodol contrast into the lymphatics may add to the apparent circumvention of the contrast medium. In patients with obstruction to lymph flow from congenital, inflammation, tumor, amd trauma etiologies the flow from the lower extremities may be demonstrated as perivascular stasis, extravasation, and dermal backflow in the lower extremities (Collins et al., 1986). Retrograde injections of saline and ethiodol into pulmonary lymphatics should reveal a variable demonstration of the lymphatics of the lung.

The authors' original approach was to select a lymph node that could be successfully cannulated and develop a model to demonstrate how the lymphatics of the lung could be successfully cannulated and identified (Fig. 13). When the saline was injected into the lymph node, the node enlarged. Peribronchial and visceral pleural lymphatics dilated. Venous communication was demonstrated between the node and the right middle lung bronchus (Fig. 7). Visually, the retrograde ethiodol contrast injections correlated with the saline injections (Figs. 4–6), demonstrating communication between the visceral pleural lymphatics. However, since the con-

trast injections demonstrated venous communication from direct needle placement, we chose to cannulate the lymphatics for detailed demonstration. When ethiodol contrast was injected into the peribronchial lymphatics and lymph nodes (Figs. 8a, b), communication between the two lungs was demonstrated (Fig. 14). This was documented under fluoroscopy. Coronal MRI demonstrated the peribronchial lymphatics in the right upper lung (Figs. 9a, b).

A modified diagram of the anatomy of the lymphatic drainage of a portion of a lung lobule and the pleura is demonstrated in Figure 15. This diagram is adopted from a previous study by Miller (1947). The diagram illustrates the communication of the visceral pleural lymphatics with the interlobular septal lymphatics and with the peribronchial lymphatics. The close proximity of the lymphatics to the bronchial walls and pulmonary veins illustrates how extravasation may occur following the rupture of peribronchial lymphatics (Fig. 12). In a previous report by Clark and Clark (1937), he stated that lymphatic capillary plexuses are abundant in the mucuous membranes of the respiratory system. Perhaps the extravasation of the ethiodol contrast medium occurred from the lymphatic capillary plexuses within the very vascular bronchial mucosa.

The authors would like to emphasize that the lymph system is contiguous with the vascular system of the lung as demonstrated in Figure 1. The lymph system is a closed system like the vascular system. The lymph flow is dependent on the elasticity and pumping action of the lung. The flow of lymph in the extremities depends upon the contraction and the relaxation of the muscles. If the lungs are scarred from chronic infections, radiation therapy, and/or toxic agents, the lymph flow is disrupted. Since tumors and infections are spread by the lymph system in the extremities, alternate pathways may occur in the lung when the normal flow is obstructed. Thoracic surgical resections may leave cells within severed lymphatics and thus allow recurrences at the site and/or distal to the surgical resection. Likewise, primary lesions in one lung may spread to the opposite lung by collateral lymph circulation. Lymphatics which are cut will lose lymph fluid into the pleural space.

The cannulation of the pulmonary lymphatics will assist in decreasing the postoperative complications of pleural effusions and may diminish complications following heart and lung transplantation. The successful cannulation of the lung lymphatics as in our model may contribute to direct lymph collection for research. The authors intend to investigate the lymph flow of other organs.

REFERENCES

Clark, E.R., R.L. Clark 1937 Observations on isolated lymphatic capillaries in the living mammal. Am J. Anat., *62:*59–62.

Collins, J.D., S. Furmanski, D. Burwell, and R. Steckel 1972a Minimal detectable pleural effusion: A Roentgen pathology model. Radiology, *105:*49–51.

Collins, J.D., S. Furmanski, R.J. Steckel, and H. Snow 1972b Minimal calcification demonstrable in pulmonary nodules: A Roentgen pathology model. Radiology, *105:*51–53.

Collins, J.D., L.W. Bassett, H. Snow, N.A. Ross, and T. Patim 1986 False positive thromboscintigram resulting from Lymphedema: A roentgen pathological model. J. Natl. Med. Assoc., *78:*875–881.

Collins, J.D., M.L. Shaver, P. Batra, and K. Brown 1989 Nerves on magnetic resonance imaging. J. Natl. Med. Assoc., *81:*129–134.

Collins, J.D., P. Batra, K. Brown, M.L. Shaver 1990 Anatomy of the lymphatic drainage as displayed by the plain x-ray and magnetic resonance imaging. Anat. Rec. *226*:21A.

Hoffman, R.R., R. Wankmuller, and L. Rigler 1966 A fallacious sign of intraperitoneal fluid. Radiology, *87*:845–847.

Miller, W.S. 1947 The Lung, 2nd Ed. Springfield, IL: Thomas.

Moskowitz H., R.T. Platt, R. Schachar, and H. Mellins 1973 Roentgen visualization of minute pleural effusion. Radiology, *109*:33–35.

Towers, B. 1968 The Fetus and Neonate. Vol. II, Chapter IV. London: Academic press.

Trapnell, D.H. 1963 The peripheral lymphatics of the lung. Br. J. Radiol. *36*:660–672.

Weidner, W.A., R.M. Steiner 1971 Roegentenographic demonstration of intrapulmonary and pleural lymphatics during Lymphangiography. Radiology, *100*:533–538.

Willis, T. 1675 The Operations of Medicines in Human Bodies (English translation 1684). London: p. 6.